Acta Geochim (2019) 38(5):627–641
https://doi.org/10.1007/s11631-019-00327-z

ORIGINAL ARTICLE

Geochemistry and sediment in the main stream of the Ca River basin, Vietnam: weathering process, solute-discharge relationships, and reservoir impact

Ho Thi Phuong[1] · Kenji Okubo[2] · Md. Azhar Uddin[2]

Received: 24 November 2018 / Revised: 6 February 2019 / Accepted: 26 February 2019 / Published online: 16 March 2019

Abstract In this study, we investigated the chemical composition of dissolved solids in the Ca River basin, North-Central Vietnam. Water samples were collected from August 2017 to July 2018 at three hydrological stations located in the main stream of the Ca River. Carbonate weathering was found as the dominant process controlling the water chemistry in that area. The average concentrations of dissolved solids generally decreased from upstream to downstream, resulting in low concentrations of the major ions in the downstream basin. Variations in the concentrations of major chemical ions and suspended solids at discharge were also investigated. Major chemical weathering products were found to behave chemostatically with increasing discharges upstream. However, dilution behaviors of solutes were shown in both midstream and downstream. Primary evidence shows that water storage in reservoirs impacts a variety of suspended solids and dissolved solids in the Ca River.

Keywords Ca River · Dissolved solids · Geochemistry · Carbonate weathering · Suspended solids

✉ Ho Thi Phuong
phuongmt.dhv@gmail.com

[1] School of Chemical, Biological and Environmental Technologies, Vinh University, 182, Le Duan Street, Vinh City, Nghe An, Vietnam

[2] Graduate School of Environmental and Life Science, Okayama University, 3-1-1, Tsushima-Naka, Kita-ku, Okayama 700-8530, Japan

1 Introduction

The natural chemical compositions and transport fluxes in rivers depend on multiple environmental factors such as sources (lithosphere, atmosphere, biosphere), sinks (vegetation uptake, settling), rate-controlling factors (temperature, water circulation), and drainage basin area (Meybeck 1994; Milliman and Farnsworth 2011). Atmospheric pollution and human activity can have significant effects on the natural geochemistry of river basins (Chetelat et al. 2008; Li et al. 2009; Li and Zhang 2008; Roy et al. 1999). Detailed geochemical studies have quantified major ion compositions (Li and Zhang 2008; Maharana et al. 2015), weathering processes (Chetelat et al. 2008; Sarin et al. 1989), long-term fluxes (Negrel et al. 2007; Sarin et al. 1989), and controlling factors in solute exports from various scales of basins (Godsey et al. 2009; Musolff et al. 2015). Some have researched natural river geochemistry, where basins with minimal human activity—such as hilly headwater basins (Bruijnzeel 1983) and unpolluted or less-polluted river basins (Meybeck 1994)—were considered. However, establishing natural background values is challenging because most major rivers are already polluted or exposed to long-range transport of atmospheric pollutants (Meybeck and Helmer 1989).

Rivers in Vietnam, like many other rivers around the world, have been impacted by economic development. Reservoirs of various sizes have been constructed along the rivers for power generation, water supply, and flood control (Amos et al. 2017). In addition, other anthropogenic activities (e.g., intensive agriculture, land-use change, and industrial development) can have significant impacts on how natural river materials move. However, geochemical data for Vietnamese rivers are sparse. Thus, we investigated the geochemistry of the Ca River, one of the large

basins in north-central Vietnam, covering an area of 27,200 km^2. Major ion chemistries were determined at sites upstream of the reservoirs, which were primarily under forest cover, and at sites mid- and downstream, below the reservoirs. Weathering processes controlling the major geochemistry were also determined. Additionally, variations in the concentrations of major chemical ions and suspended solids in the discharge were investigated.

2 Study area

The Ca River is an international river located between 18°15′00″N to 20°10′30″N and 103°45′20″E to 105°15′20″E (Fig. 1). The basin covers 27,200 km^2, including 17,730 km^2 in Vietnam's territory and 9470 km^2 in Laos. The main river originates from Mt. Muong Khut and Muong Lap (1800–2000 m) in Laos, flows from northwest to southeast, enters into the Nghe An, Thanh Hoa, and Ha Tinh provinces of Vietnam, and flows out to the Eastern Sea at the Hoi estuary. Total river length is 531 km, of which 170 km runs through Laos and 361 km is in Vietnam. Forests in the Ca River basin are largely located upstream of three Laos provinces (Bolikhamxay, Xieng Khouang, and Houaphanh). In Vietnam, forests are concentrated north, northwest, and southwest of the basin at elevations of 150–1500 m (IWRP 2012). The catchment is covered primarily by forest (44%) and agricultural crops (18%) (Chikamori et al. 2012). Area soils are formed from parent rocks, Ferralsol in particular (83.51%) (IWRP 2012; Nauditt and Ribbe 2017). Other soil types are Fluvisol and Acrisol. The Ca River basin is located in a monsoon climate, and rainfall is distributed over the year, which has two distinct seasons: the dry season and the rainy season. In the upper reaches of the river, the rainy season is from May to October, but downstream, it is from June to November.

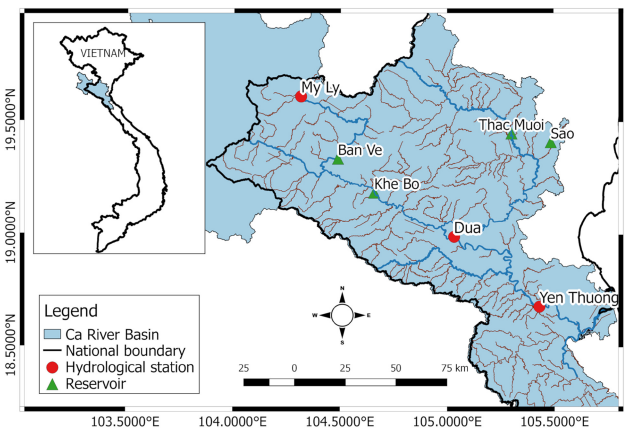

Fig. 1 Map of the Ca River basin

Average annual precipitation in the basin is 1100–2500 mm.

Multiple reservoirs have been constructed in the Ca River basin, namely Ban Ve, Khe Bo, Thac Muoi, and Sao reservoirs. These multi-purpose reservoirs are used for hydropower generation, water supply, irrigation, and flood and drought control. Ban Ve is the largest among them and is located at approximately 100 m elevation. Its gross capacity is 1835 × 10^6 m^3, and its effective capacity is 1383 × 10^6 m^3.

Samples were obtained from the main stream of the Ca River at My Ly (104°18′54″E and 19°36′51″N), Dua (105°02′20″E and 18°59′20″N), and Yen Thuong (105°23′00″E and 18°41′10″N). My Ly is located approximately 215 m above the Ban Ve reservoir (70 km). It covers 1190 km^2 or 4.4% of the total drainage basin. Located in the high mountains and covered primarily by forest, the My Ly basin is sparsely populated and is subject to little human impact. Both Dua and Yen Thuong are downstream of all reservoirs, covering 20,800 km^2 and 23,000 km^2 (76.5% and 84.6% of the river basin), respectively. Both are strongly influenced by human activity (e.g., agriculture and mining activities). Additionally, water storage and reservoir operations impact the Ca River and its resources.

3 Sampling and analytical methods

From August 2017 to July 2018, 121 water samples were collected from three hydrological stations in the main stream of the Ca River basin. During the flood season, water samples were collected four to six times monthly, and during the dry season, they were collected one to four times monthly. Samples were representative of the range of discharge rates.

Each sample of 2 L, collected from an average depth of 10 cm at the river bank, was placed in high-density polyethylene containers then immediately cooled and maintained at a low temperature until analysis. Concentrations of the major cations (Ca^{2+}, Mg^{2+}, Na^+, and K^+), anions (HCO_3^-,SO_4^{2-}, Cl^-, NO_3^-, and PO_4^{3-}), and dissolved silica (SiO_2) were determined in the laboratory. Cation and most anion concentrations were found using ion chromatography (Shimadzu, Japan). Dissolved silica and phosphate were measured using a DR900 (HACH) colorimeter. Water samples were filtered through pre-washed 0.45-μm Millipore membrane filters before ion concentrations were determined. Additionally, the concentration of suspended solids was determined by filtering 100 mL sample through a 0.45-μm membrane filter (Whatman). Finally, the total

concentration of all dissolved solids was the sum of the major elements plus dissolved silica.

4 Results and discussion

4.1 Contributions of chemical compositions

The concentration of each major chemical in the main stream of the Ca River basin is given in Table 1. Total dissolved solids (TDS) varied from 77 to 205 mg/L, averaging 144 mg/L, higher than the world average, 100 mg/L (Milliman and Farnsworth 2011). The average value for TDS is comparable to that reported for the Hong (176 mg/L) in Vietnam, but it is lower than that reported for the Son in India (227 mg/L) and the Upper Han River in China (248 mg/L) (Li and Zhang 2008; Maharana et al. 2015; Moon et al. 2007). Compared with the rivers draining in areas dominated by silicate rock, such as the upper Ganjiang (63 mg/L) and rivers in the Southeast Coastal Region of China (75.2 mg/L), TDS in the Ca River is much higher (Liu et al. 2018; Ji and Jiang 2012). However, it is much lower compared to the Huanghe (557 mg/L) and Tarim (1000 mg/L), both of which drain in areas dominated by evaporite dissolution (Fan et al. 2014; Xiao et al. 2012). Bedrock lithology plays a critical role in controlling the character and quantity of the total delivered (Meybeck 1987; Milliman and Farnsworth 2011). Human activity also significantly influences TDS values [e.g., in the Liao River of China (400 mg/L) and several European rivers (Ding et al. 2016; Milliman and Farnsworth 2011)].

The total cationic charge ($Tz^+ = 2Ca^{2+} + 2Mg^{2+} + K^+ + Na^+$) ranged from 1145–2981 μeq/L, averaging 2119 μeq/L. The total anionic charge ($Tz^- = HCO_3^- + 2SO_4^{2-} + Cl^- + NO_3^- + 3PO_4^{3-}$) ranged from 811 to 2271 μeq/L, averaging 1567 μeq/L. The extent of $Tz^+ - Tz^-$ charge imbalance, characterized by the normalized inorganic charge balance [$NICB = (Tz^+ - Tz^-)/Tz^+$], is related to the contributions of other anions (Li et al. 2009; Ji and Jiang 2012).

Calcium was the dominant cation, ranging in concentration from 381 to 1005 μM, accounting for an average of 62.0% of the total cation charge. Magnesium followed, ranging from 102 to 368 μM, accounting for an average of 23.2% of the total cation charge, then sodium (12.3%) and potassium (2.4%) followed. Bicarbonate was the dominant anion, ranging from 600 to 2039 μM, accounting for 84.4% of the total anion charge. Chloride and sulfate together comprised 12.6% of the total anion charge in nearly equal proportions. Nitrate and phosphate contributed negligible proportions (2.7 and 0.3%, respectively).

Dissolved Si ranged in concentration from 133 to 250 μM, averaging 202 μM, comprising an average of 8.6% of the TDS. It ranked third in abundance after HCO_3^- (55.8%) and Ca^{2+} (18.3%). Compared to other major ions, dissolved Si was relatively independent of lithology, remaining constant between 80 and 160 μmol/L SiO_2(except in streams draining volcanic rocks, where it reaches 350 μmol/L SiO_2) (Meybeck 1987). Dissolved Si content is, however, controlled by the climate (temperature and rainfall) (White and Blum 1995).

4.2 Spatial and seasonal variations of major solutes and suspended solids

The total concentrations of major solutes at My Ly ranged from 142 to 205 mg/L, averaging 168 mg/L. At Dua, TDS varied from 85 to 171 mg/L, averaging 138 mg/L. On the other hand, the TDS value at Yen Thuong ranged from 77 to 167 mg/L, averaging 128 mg/L. Generally, the total solute concentration decreased from upstream to downstream, consistent with decreased concentrations of the major ions Ca^{2+}, Mg^{2+}, Na^+, Cl^-, HCO_3^-, SO_4^{2-}, and SiO_2 in the downstream basin. The observed spatial variations in solute concentrations in the main stream of the Ca River could be related to the effects of tributary inflows, resulting in dilution. A downstream trend in K^+ concentration was not significant, reflecting its conservative behavior in the basin. An increase in NO_3^- concentration in the downstream basin might have been from anthropogenic sources such as agricultural activity and untreated sewage (Maharana et al. 2015).

The study period was divided into two sub-periods: the wet season (June to November for Dua and Yen Thuong and May to October for My Ly) and the dry season (December to May and November to April, respectively) (Fig. 2). Trends in seasonal solute variations were similar between Dua and Yen Thuong. The concentrations of almost all tested ions increased from the wet to dry seasons, indicating the dilution effect of greater atmospheric precipitation during the rainy season. For that reason, at Dua and Yen Thuong, the total solute concentration increased from the wet to dry seasons. At My Ly, however, TDS decreased slightly from the wet to dry seasons, a result of decreased concentration in the major ion HCO_3^-. Other elements remained constant when comparing the two seasons. Phosphate concentration increased in the wet season at all stations, indicating the contribution of organic matter degradation (at My Ly) or human activity (at Dua and Yen Thuong).

Normally, suspended sediment concentration (SSC) decreases from upstream to downstream and from the wet to dry seasons (Fig. 2). In our case, it greatly varied from

Table 1 Chemical compositions of the rivers in the Ca River basin

Stations	Date	Discharge m^3/s	Na^+ mg/L	K^+ mg/L	Ca^{2+} mg/L	Mg^{2+} mg/L	Cl^- mg/L	SO_4^{2-} mg/L	HCO_3^- mg/L	NO_3^- mg/L	PO_4^{3-} mg/L	SiO_2 mg/L	NIBC	TSS mg/L
My Ly	13/08/2017	172	4.65	1.30	30.43	7.89	1.15	4.28	120.80	–	0.13	12	0.12	54
	20/08/2017	154	13.87	1.73	18.74	6.68	7.93	6.00	97.60	–	0.16	13	0.08	41
	27/08/2017	198	14.20	2.76	24.51	7.90	12.24	6.76	107.40	–	0.14	12	0.12	81
	03/09/2017	152	6.69	1.70	29.40	7.37	2.89	4.16	95.16	–	0.17	13	0.28	183
	10/09/2017	148	6.29	1.83	28.86	8.55	2.82	5.45	101.30	–	0.15	13	0.25	59
	16/09/2017	400	5.97	1.83	22.74	6.74	3.11	4.61	100.00	2.82	0.25	13	0.06	576
	17/09/2017	380	4.39	1.64	30.54	6.92	2.19	5.93	118.30	2.54	0.19	12	0.07	502
	24/09/2017	108	5.46	2.30	24.34	5.45	3.69	5.78	102.50	1.78	0.13	13	0.01	46
	01/10/2017	128	7.67	1.39	26.86	8.87	3.79	3.86	96.38	0.85	0.17	13	0.27	25
	08/10/2017	132	13.63	3.16	27.55	7.67	10.65	6.14	91.50	10.11	0.17	13	0.22	46
	22/10/2017	348	11.78	1.78	28.42	6.94	5.45	9.46	93.94	1.06	0.20	13	0.25	15
	05/11/2017	328	8.19	1.63	26.99	7.56	3.85	5.43	96.38	2.23	0.12	12	0.22	5
	12/11/2017	132	4.65	1.17	27.82	7.09	1.01	4.56	97.60	0.38	0.19	13	0.21	6
	19/11/2017	132	6.65	2.31	28.51	8.66	2.32	5.43	93.94	0.93	0.12	13	0.30	5
	26/11/2017	130	4.93	1.31	28.23	7.64	0.62	4.97	97.60	0.54	0.11	14	0.24	7
	03/12/2017	130	6.77	2.23	26.98	8.27	3.08	5.87	96.38	2.14	0.13	13	0.23	3
	10/12/2017	132	6.24	1.25	23.11	7.33	0.57	5.32	90.28	5.39	0.12	13	0.18	7
	17/12/2017	132	8.38	2.20	25.04	7.24	3.16	4.87	96.38	2.27	0.10	14	0.20	9
	24/12/2017	129	4.57	1.21	24.65	6.11	1.97	4.83	93.94	1.29	0.04	13	0.12	3
	30/12/2017	129	5.64	1.90	29.36	7.72	3.25	5.50	97.60	1.87	0.15	13	0.23	12
	21/01/2018	80	4.76	1.62	27.79	5.23	2.47	4.25	79.30	4.05	0.19	12	0.26	5
	28/01/2018	50	11.08	1.68	29.94	8.95	6.60	6.28	98.82	6.30	0.08	12	0.26	7
	04/02/2018	42	9.54	1.87	28.24	8.92	5.97	6.52	96.38	2.43	0.11	13	0.26	3
	04/03/2018	40	6.35	1.93	26.38	6.44	3.70	3.94	102.50	3.12	0.04	13	0.12	4
	11/03/2018	40	7.12	1.78	31.39	8.20	3.39	5.27	102.50	1.98	0.11	13	0.26	23
	01/04/2018	40	10.83	2.49	30.75	8.15	4.98	6.28	97.60	1.02	0.10	14	0.31	39
	08/04/2018	40	5.06	2.14	31.51	8.03	1.43	5.90	97.60	1.48	0.23	14	0.28	360
	16/04/2018	72	8.62	2.01	32.65	8.33	4.50	5.06	98.82	3.27	0.09	12	0.30	265
	29/04/2018	48	13.17	3.08	27.06	7.53	8.85	6.62	87.84	6.09	0.17	14	0.26	632
	06/05/2018	94	5.96	2.27	26.77	7.29	2.00	4.89	95.16	2.39	0.20	12	0.22	410
	13/05/2018	72	5.02	2.13	34.24	7.74	1.49	6.20	98.82	1.01	0.23	15	0.31	414
	27/05/2018	60	5.15	2.17	30.41	6.07	2.28	4.94	81.74	1.64	0.36	12	0.33	200
	03/06/2018	160	6.70	2.31	34.31	8.37	3.41	5.67	109.80	3.45	0.40	12	0.24	536
	17/06/2018	240	4.49	3.14	40.27	8.46	2.00	6.12	124.40	2.37	0.33	13	0.24	3727
	24/06/2018	87	4.29	1.47	35.91	8.02	0.94	5.25	112.20	0.96	0.11	12	0.25	338
	08/07/2018	72	5.25	1.64	28.60	7.51	1.23	2.62	103.70	0.31	0.12	12	0.22	197
	16/07/2018	160	5.59	2.78	23.19	5.50	3.88	5.97	106.10	2.57	0.08	12	− 0.05	387
	22/07/2018	2100	3.33	1.27	26.42	5.95	2.86	7.35	89.06	5.35	0.16	12	0.10	2310

Table 1 continued

Stations	Date	Discharge m^3/s	Na^+ mg/L	K^+ mg/L	Ca^{2+} mg/L	Mg^{2+} mg/L	Cl^- mg/L	SO_4^{2-} mg/L	HCO_3^- mg/L	NO_3^- mg/L	PO_4^{3-} mg/L	SiO_2 mg/L	NIBC	TSS mg/L
Dua	06/08/2017	869	4.16	1.75	23.39	4.35	2.68	2.87	84.18	–	0.20	12	0.13	77
	14/08/2017	463	3.47	1.45	23.89	5.12	1.24	3.20	85.40	–	0.19	13	0.16	57
	20/08/2017	860	8.65	1.97	23.04	4.84	5.47	3.88	63.44	–	0.13	12	0.35	106
	27/08/2017	882	3.76	1.83	26.77	4.98	2.43	3.30	78.08	–	0.19	11	0.27	85
	04/09/2017	565	3.99	1.54	21.73	5.23	2.30	3.29	70.76	–	0.15	12	0.25	58
	10/09/2017	562	3.94	1.43	24.98	5.49	1.92	3.41	73.20	–	0.18	11	0.30	42
	17/09/2017	2688	3.77	1.83	18.41	3.86	2.37	3.26	51.24	3.60	0.25	10	0.28	621
	24/09/2017	610	4.59	2.10	23.47	5.39	2.06	4.11	75.64	3.35	0.15	12	0.23	62
	01/10/2017	749	10.14	1.63	26.80	5.78	10.82	3.06	81.74	2.14	0.14	13	0.24	33
	08/10/2017	1241	6.13	2.25	20.97	4.55	4.72	3.60	63.44	5.79	0.20	12	0.23	174
	10/10/2017	1772	3.45	1.70	18.75	3.09	2.51	2.71	54.90	3.91	0.19	11	0.21	395
	11/10/2017	3564	2.91	1.77	16.98	3.40	2.41	2.51	61.00	3.81	0.18	12	0.09	411
	12/10/2017	4393	2.55	1.82	16.08	2.89	2.00	2.58	43.90	4.43	0.24	9	0.24	465
	22/10/2017	700	8.65	1.76	26.22	6.37	5.06	5.68	78.08	3.78	0.17	14	0.29	40
	05/11/2017	336	8.22	1.89	27.37	6.22	4.34	3.99	80.52	3.42	0.10	13	0.31	17
	12/11/2017	440	9.51	2.30	27.86	6.68	5.99	4.34	84.18	3.12	0.16	14	0.30	8
	20/11/2017	283	4.80	1.97	27.70	6.18	1.97	4.20	78.08	2.40	0.13	13	0.32	36
	26/11/2017	246	3.73	1.45	24.71	5.30	0.97	4.21	80.52	2.38	0.14	14	0.21	17
	03/12/2017	259	4.65	1.59	24.31	5.39	1.92	3.75	75.64	2.69	0.14	14	0.25	12
	10/12/2017	494	4.28	1.57	23.88	5.30	1.71	3.73	84.18	3.00	0.11	13	0.16	10
	18/12/2017	195	14.05	4.47	27.62	7.82	8.94	10.08	79.30	5.97	0.08	13	0.32	8
	24/12/2017	170	4.98	1.45	24.14	5.45	2.22	4.41	81.74	2.08	0.09	13	0.20	4
	31/12/2017	240	8.64	2.55	25.80	7.01	7.62	4.84	78.08	4.61	0.13	13	0.27	5
	21/01/2018	289	5.66	1.59	27.85	6.08	2.45	4.00	81.70	1.95	0.12	11	0.30	9
	27/01/2018	169	8.85	2.20	30.37	7.28	6.93	4.72	93.94	2.93	0.06	11	0.26	12
	04/02/2018	154	4.37	1.51	28.35	6.04	1.23	4.37	86.62	1.42	0.14	13	0.27	8
	04/03/2018	56	4.65	1.86	27.27	5.55	2.68	3.75	87.84	2.82	0.04	12	0.21	8
	11/03/2018	185	4.43	1.62	30.77	6.45	1.53	4.56	87.84	1.97	0.13	12	0.30	8
	02/04/2018	117	10.39	2.39	31.33	7.77	5.79	5.52	86.60	3.27	0.08	12	0.35	3
	07/04/2018	345	4.50	1.62	31.64	6.29	2.37	4.45	86.62	1.64	0.08	12	0.31	139
	17/04/2018	300	5.59	1.86	31.70	6.80	2.74	4.34	86.62	2.11	0.10	12	0.33	6
	01/05/2018	275	4.31	1.92	28.14	5.79	2.10	4.34	80.52	1.81	0.09	13	0.29	14
	06/05/2018	294	7.28	2.04	28.62	6.64	4.79	3.60	73.20	3.80	0.23	12	0.37	76
	13/05/2018	339	8.69	2.21	27.00	5.59	5.69	4.66	74.42	4.46	0.19	12	0.31	44
	20/05/2018	356	4.67	2.01	28.29	6.38	2.14	5.20	73.00	2.21	0.19	11	0.36	557
	27/05/2018	252	4.38	2.03	29.49	5.64	2.09	3.05	76.86	1.05	0.20	11	0.35	9
	03/06/2018	319	5.87	2.71	29.79	5.79	3.70	4.27	84.18	1.43	0.35	11	0.30	13
	17/06/2018	316	6.95	2.37	27.14	5.46	4.99	4.70	73.20	2.63	0.13	13	0.31	157
	24/06/2018	420	4.08	1.84	25.76	5.22	1.92	3.90	70.76	1.40	0.13	12	0.32	40
	08/07/2018	455	8.85	2.34	30.31	6.70	4.82	5.43	84.18	2.30	0.19	12	0.33	13
	16/07/2018	747	5.69	1.36	22.24	2.87	5.69	3.29	84.18	2.26	0.10	11	− 0.01	72
	22/07/2018	4210	2.22	1.79	20.71	4.30	1.26	4.58	70.76	3.83	0.26	11	0.11	867

Table 1 continued

Stations	Date	Discharge m^3/s	Na^+ mg/L	K^+ mg/L	Ca^{2+} mg/L	Mg^{2+} mg/L	Cl^- mg/L	SO_4^{2-} mg/L	HCO_3^- mg/L	NO_3^- mg/L	PO_4^{3-} mg/L	SiO_2 mg/L	NIBC	TSS mg/L
Yen Thuong	06/08/2017	752	3.39	1.44	21.74	4.15	1.51	3.27	74.42	–	–	–	0.17	158
	14/08/2017	430	3.39	1.60	22.97	4.69	1.72	3.20	86.62	–	0.23	12	0.10	77
	20/08/2017	862	3.97	1.72	18.73	4.19	1.98	2.91	62.22	–	0.13	11	0.24	187
	27/08/2017	750	4.80	1.97	24.02	4.46	3.65	3.56	68.32	–	0.25	11	0.29	117
	04/09/2017	475	3.80	1.82	24.77	4.27	3.02	3.03	65.88	–	0.14	11	0.31	107
	10/09/2017	514	3.83	1.58	25.53	4.98	2.29	3.56	68.32	–	0.14	12	0.33	66
	17/09/2017	2910	3.42	1.80	15.36	2.95	3.02	2.98	37.82	4.14	0.18	9	0.30	343
	18/09/2017	2625	6.42	1.80	18.03	2.48	5.34	2.29	50.02	5.28	0.20	10	0.22	369
	24/09/2017	750	5.26	2.17	17.98	4.73	3.59	4.11	53.68	3.68	0.13	12	0.28	85
	01/10/2017	690	5.16	1.91	27.33	5.17	4.23	3.72	75.64	2.57	0.15	12	0.28	95
	08/10/2017	2045	4.43	2.09	17.08	3.16	3.81	2.89	46.36	4.61	0.20	9	0.26	75
	10/10/2017	3150	2.58	2.17	15.29	2.60	2.58	3.10	36.60	4.08	0.25	8	0.29	200
	12/10/2017	4422	2.88	2.07	15.99	2.65	2.47	2.90	51.20	4.10	0.20	10	0.13	186
	22/10/2017	735	5.53	1.63	25.39	4.72	3.01	4.19	65.88	3.34	0.16	13	0.32	56
	05/11/2017	480	5.65	1.65	27.58	5.57	3.02	4.31	73.20	2.93	0.12	13	0.33	18
	12/11/2017	420	6.03	1.84	26.64	5.22	3.54	3.56	82.96	2.63	0.14	13	0.24	22
	20/11/2017	400	4.44	1.22	25.01	4.56	2.88	4.37	67.01	2.38	0.15	13	0.29	17
	27/11/2017	327	3.86	1.45	22.46	4.69	1.81	3.25	58.56	2.64	0.15	13	0.34	7
	03/12/2017	375	8.50	2.00	21.65	6.42	6.69	4.70	69.54	4.58	0.12	12	0.26	4
	10/12/2017	260	5.61	1.71	24.48	5.69	3.42	4.34	57.34	3.52	0.10	13	0.40	13
	18/12/2017	326	5.79	2.14	24.39	5.38	4.50	5.03	69.54	2.72	0.09	13	0.28	10
	24/12/2017	287	7.04	1.84	24.89	6.65	3.79	4.48	76.86	4.08	0.07	13	0.29	6
	31/12/2017	255	4.60	1.68	26.27	5.37	2.64	3.80	74.42	2.26	0.13	12	0.29	13
	21/01/2018	310	6.72	1.45	28.38	8.43	2.63	5.37	95.20	1.18	0.12	12	0.27	5
	27/01/2018	235	7.45	3.49	27.94	6.19	2.88	3.85	64.66	2.05	0.04	11	0.46	9
	04/02/2018	275	8.30	2.09	28.76	6.84	5.80	5.67	73.20	3.77	0.12	11	0.36	6
	04/03/2018	260	4.18	1.73	27.21	5.33	2.38	4.35	78.08	2.23	0.03	12	0.27	3
	11/03/2018	180	4.89	2.18	30.04	6.16	3.30	4.87	78.08	4.76	0.08	11	0.32	23
	02/04/2018	148	10.15	2.34	30.54	7.58	7.63	5.80	57.30	2.97	0.06	11	0.50	14
	07/04/2018	120	5.21	1.58	30.06	6.55	2.68	4.24	82.96	2.09	0.11	12	0.32	18
	17/04/2018	142	4.72	1.85	29.25	6.25	1.88	4.05	73.20	1.92	0.20	13	0.38	7
	06/05/2018	119	8.91	2.17	23.71	5.69	6.59	4.78	62.22	5.48	0.25	11	0.33	211
	13/05/2018	335	6.60	2.05	27.64	5.50	4.01	4.61	73.20	3.64	0.25	12	0.32	55
	20/05/2018	180	5.29	2.87	27.21	5.81	2.66	5.58	62.00	2.82	0.21	12	0.41	33
	28/05/2018	176	7.10	2.30	31.14	7.70	3.69	8.85	93.94	2.04	0.22	10	0.27	25
	02/06/2018	149	5.22	2.05	27.49	5.51	2.62	3.80	74.42	2.13	0.25	12	0.33	13
	17/06/2018	240	11.81	3.21	28.47	8.15	9.51	8.73	73.20	3.16	0.21	13	0.36	12
	24/06/2018	370	5.07	1.78	24.02	5.48	2.26	4.20	75.64	0.90	0.11	12	0.26	24
	08/07/2018	300	5.25	2.16	28.80	6.26	2.44	4.28	81.74	1.28	0.25	12	0.32	52
	16/07/2018	350	3.35	1.82	22.31	4.34	2.93	5.47	65.88	1.70	0.09	10	0.21	246
	22/07/2018	1410	2.32	1.24	18.13	3.27	1.37	5.56	54.90	5.95	0.13	10	0.12	228

month to month (Fig. 3), showing the opposite trend of that seen for solute concentration, except at My Ly (for example, in June and July). The highest SSCs occurred during September, October, and July at Dua and Yen Thuong (135–317 mg/L). Peak SSC occurred in June at My Ly (1534 mg/L), indicating significant erosion in the upper basin due to heavy rain.

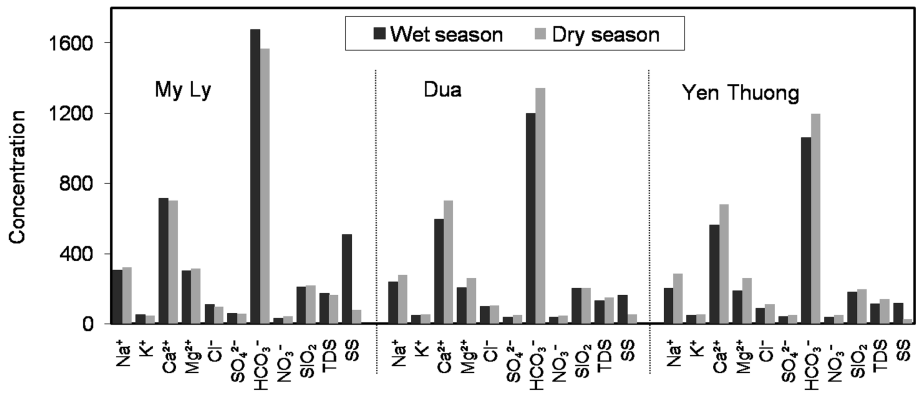

Fig. 2 Seasonal variations in the concentration of major ions (μM), TDS, and SS (mg/L)

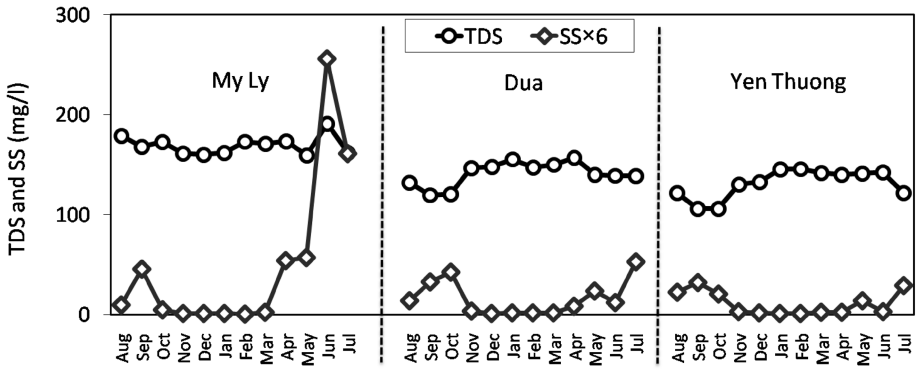

Fig. 3 Monthly variations in the concentration of TDS and SS (mg/L)

4.3 Weathering processes controlling the major ion chemistry

Major natural processes determining the ion chemistry of water can be identified by plotting variations in the weight ratio between $Na^+$and $Na^+ + Ca^{2+}$ as a function of TDS (Gibbs 1970). The sources of major ions were divided into three groups: precipitation dominance, rock dominance, and evaporation-crystallization dominance. Figure 4 shows weathering dominance for most of the samples drawn. Rock weathering controls the water composition in the Ca River basin, producing a TDS value between 77 and 205 mg/L and a $Na^+/(Na^+ + Ca^{2+})$ ratio ranging from 0.10 to 0.43.

The three primary lithologies undergoing chemical weathering were silicates, carbonates, and evaporites (Gaillardet et al. 1997). Carbonate weathering (calcite, dolomites) produces Ca^{2+}, Mg^{2+}, and HCO_3^-. Silicate weathering results in HCO_3^-, Na^+, K^+, Mg^{2+}, Ca^{2+}, and SiO_2. Evaporite dissolution results in Na^+, K^+, Cl^-, and SO_4^{2-} (Han and Liu 2001; Meybeck 1987; Sarin et al. 1989). The relationships between Ca^{2+}/HCO_3^-, $(Ca^{2+} + Mg^{2+})$/total cations, and $(Na^+ + K^+)$/total cations for the Ca River were determined to evaluate the contribution of rock weathering. The Ca^{2+} and HCO_3^- for most samples fell along a 1:1 equiline (Fig. 5a), implying that

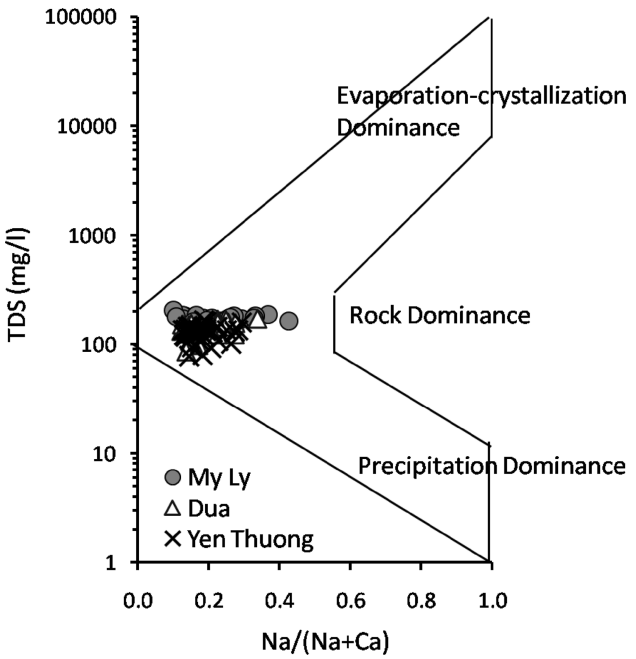

Fig. 4 The Gibbs graph of Ca River between the ratio of Na/(Na + Ca) and total dissolved solids

carbonates dissolution dominates in this drainage basin (Roy et al. 1999). The HCO_3^- is slightly more enriched than Ca^{2+} at My Ly, possibly consistent with a silicate weathering source for some of this anion (Holland 1978). The

scatter plot (Fig. 5b) of $(Ca^{2+} + Mg^{2+})$ against total cations indicates a significant contribution of these two cations (approximately 85% of the total). Any deviation of $(Ca^{2+} + Mg^{2+})$ from the 1:0.85 line was attributed to increasing proportions of $Na^+ + K^+$) (Fig. 5b, c), implying contributions from silicate weathering or evaporite dissolution (Li and Zhang 2008; Maharana et al. 2015). The correlations among geochemistry parameters and their correlations with suspended solids were investigated for each station (Table 2). The significant relationships between Ca^{2+}/Mg^{2+}, Ca^{2+}/HCO_3^-, Mg^{2+}/HCO_3^-, Ca^{2+}/TDS, Mg^{2+}/TDS, and HCO_3^-/TDS at all stations support the finding of carbonate weathering dominance in the Ca River basin. Significant correlations between SiO_2 and Na^+, K^+, or HCO_3^- were not found, implying minimal silicate weathering. However, moderate correlations between Cl^-, SO_4^{2-}, Na^+, K^+, and TDS were found, indicating that evaporite weathering was the source (Li and Zhang 2008).

The Piper diagram is widely applied to determine the classification of water on the basis of its chemical character (Maharana et al. 2015; Negrel et al. 2007; Ji and Jiang 2012). The triangular cationic fields of the Piper diagram (Fig. 6) revealed that most of the water samples fell into the Ca^{2+} field, whereas in the anion triangle, the majority fell into the HCO_3^- field. Chemical data plotted on the diamond-shaped central field revealed the dominance of the $Ca^{2+} - HCO_3^-$ type. Therefore, $Ca^{2+} - HCO_3^-$ is the dominant hydrogeochemical species in the Ca River basin. The Piper diagram for our Ca River samples is similar to that for the Son River (Maharana et al. 2015) and the upstream Huanghe River (Fan et al. 2014), dominated by carbonate weathering. However, it differs from the mid- and downstream sections of the Huanghe River (Fan et al. 2014), where evaporite dissolution dominates. They also differ from the Liao River, Daling River, Hun-Tai River (Ding et al. 2016), Ou River, and Min River (Liu et al. 2018), where silicate weathering dominates. In many

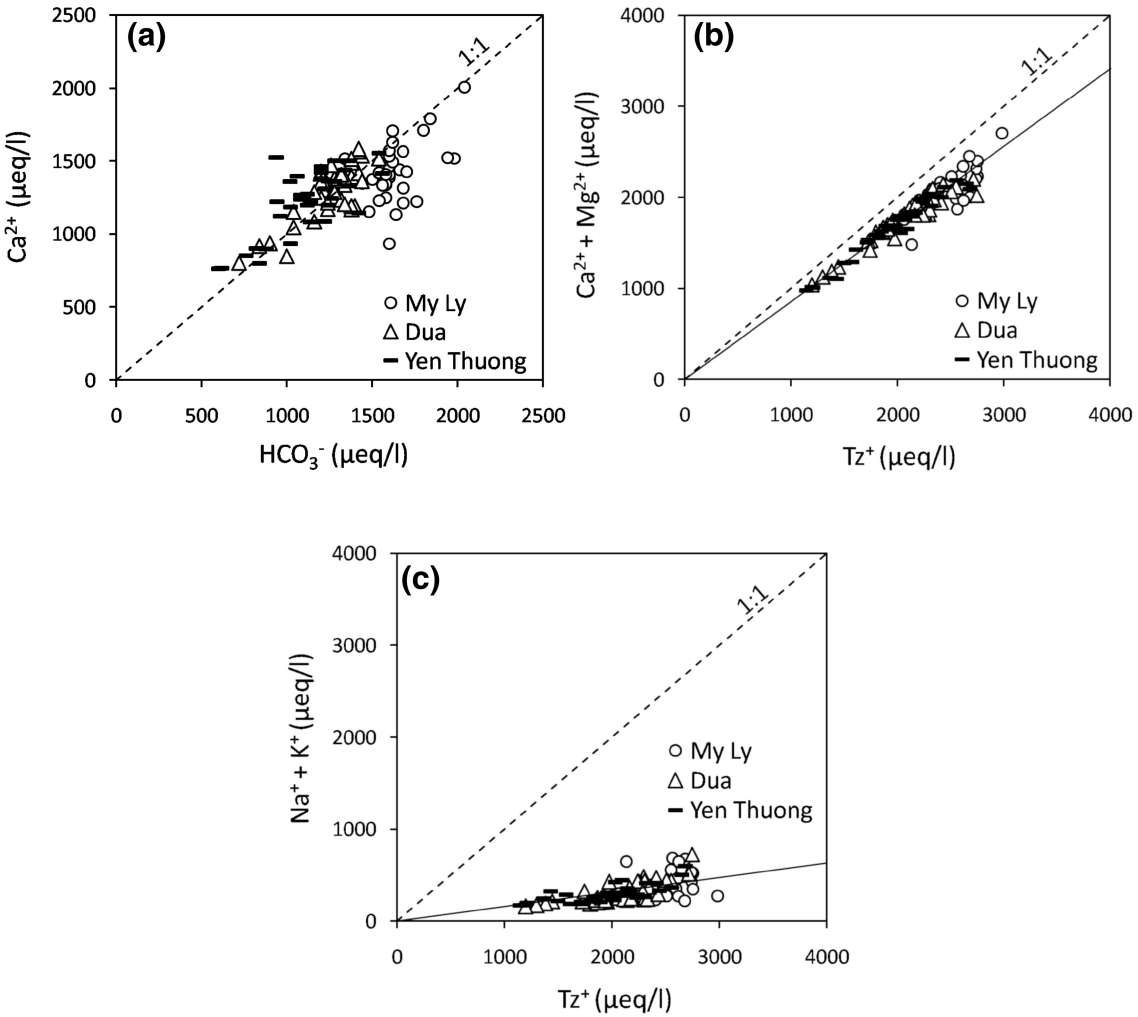

Fig. 5 Scatter plots between **a** Ca^{2+} and HCO_3^-, **b** Ca^{2+}, Mg^{2+}, and total cations, and **c** Na^+, K^+, and total cations

Table 2 Correlation matrix of measured parameters at three hydrological stations

	Na^+	K^+	Ca^{2+}	Mg^{2+}	Cl^-	SO_4^{2-}	HCO_3^-	NO_3^-	PO_4^{3-}	SiO_2	TDS	TSS
My Ly												
Na^+	1.00											
K^+	0.43**	1.00										
Ca^{2+}	− 0.30	0.16	1.00									
Mg^{2+}	0.26	0.11	0.48**	1.00								
Cl^-	0.91**	0.54**	− 0.30	0.11	1.00							
SO_4^{2-}	0.44**	0.33*	0.04	0.05	0.46**	1.00						
HCO_3^-	− 0.19	0.10	0.42**	0.30	− 0.13	− 0.04	1.00					
NO_3^-	0.49**	0.34	− 0.17	− 0.04	0.67**	0.24	− 0.25	1.00				
PO_4^{3-}	− 0.15	0.27	0.40*	0.01	− 0.10	0.12	0.06	0.00	1.00			
SiO_2	0.12	0.17	0.01	0.17	− 0.03	0.15	− 0.19	− 0.16	− 0.04	1.00		
TDS	0.33*	0.49**	0.54**	0.55**	0.37*	0.34*	0.76**	0.18	0.15	− 0.03	1.00	
TSS	− 0.27	0.28	0.43**	− 0.01	− 0.12	0.23	0.35*	0.13	0.44**	− 0.07	0.36*	1.00
Dua												
Na^+	1.00											
K^+	0.68**	1.00										
Ca^{2+}	0.45**	0.25	1.00									
Mg^{2+}	0.64**	0.47**	0.85***	1.00								
Cl^-	0.89**	0.56**	0.22	0.37*	1.00							
SO_4^{2-}	0.67**	0.77**	0.46**	0.68**	0.41**	1.00						
HCO_3^-	0.31*	0.03	0.78**	0.65**	0.16	0.33*	1.00					
NO_3^-	0.35*	0.49**	− 0.47**	− 0.10	0.39*	0.28	− 0.47**	1.00				
PO_4^{3-}	− 0.30	0.00	− 0.35*	− 0.39*	− 0.20	− 0.30	− 0.48**	0.13	1.00			
SiO_2	0.35*	0.06	0.28	0.43**	0.19	0.32*	0.45**	− 0.03	− 0.41**	1.00		
TDS	0.69**	0.40**	0.86**	0.86**	0.50**	0.62**	0.88**	− 0.19	− 0.49**	0.51**	1.00	
TSS	− 0.42**	− 0.10	− 0.59**	− 0.53**	− 0.25	− 0.18	− 0.66**	0.28	0.49**	− 0.53**	− 0.66**	1.00
Yen Thuong												
Na^+	1.00											
K^+	0.56**	1.00										
Ca^{2+}	0.50**	0.23	1.00									
Mg^{2+}	0.73**	0.34*	0.84**	1.00								
Cl^-	0.87**	0.50**	0.19	0.41**	1.00							
SO_4^{2-}	0.60**	0.39*	0.53**	0.71**	0.49**	1.00						
HCO_3^-	0.25	− 0.09	0.76**	0.70**	− 0.06	0.40**	1.00					

Table 2 continued

	Na^+	K^+	Ca^{2+}	Mg^{2+}	Cl^-	SO_4^{2-}	HCO_3^-	NO_3^-	PO_4^{3-}	SiO_2	TDS	TSS
NO_3^-	0.02	− 0.03	− 0.55**	− 0.45**	0.31	− 0.16	− 0.58**	1.00				
PO_4^{3-}	− 0.08	0.09	− 0.19	− 0.24	0.02	− 0.06	− 0.12	0.16	1.00			
SiO_2	0.29	− 0.13	0.55**	0.51**	0.04	0.15	0.54**	− 0.41*	− 0.23	1.00		
TDS	0.59**	0.16	0.90**	0.89**	0.28	0.63**	0.92**	− 0.48**	− 0.15	0.59**	1.00	
TSS	− 0.37*	− 0.17	− 0.72**	− 0.72**	− 0.07	− 0.36*	− 0.60**	0.51**	0.30	− 0.69**	− 0.69**	1.00

**Correlation is significant at the 0.01 level

*Correlation is significant at the 0.05 level

watersheds around the world, carbonate weathering play an important role in controlling river water chemistry because carbonate is more susceptible to weathering than silicate (Fan et al. 2014; Roy et al. 1999).

4.4 Variations in major solute concentrations at discharge

The relationships between solute concentration and its discharge were investigated at each hydrological station. Concentrations of the weathering-derived solutes were plotted against instantaneous discharge on logarithmic axes (Fig. 7), yielding the approximate relationships between concentration and discharge using a power law (Baronas et al. 2017; Herndon et al. 2015; Musolff et al. 2015):

$$C = a \times Q^b \quad (1)$$

where C is solute concentration, Q is discharge, and a and b are constants. The exponent b is the slope of the $C - Q$ relationship on logarithmic axes. When concentration does not change with changing discharge, the relationship is said to be chemostatic (Moatar et al. 2017; Musolff et al. 2015). When this is the case, b is between −0.1 and 0 (Herndon et al. 2015; Hunsaker and Johnson 2017). When discharge increases, solute concentrations can either increase (enrichment behavior, $b > 0$) or decrease (dilution behavior, $b < -0.1$), and the relationship is said to be chemodynamic (Herndon et al. 2015).

Our results show that the upstream catchment (My Ly) behaved chemostatically for the major chemical weathering products except for Na^+ ($b = -0.11$), NO_3^- ($b = 0.11$), and PO_4^{3-} ($b = 0.15$). The large store/high production rate of weathering products can lead to chemostatic behavior for major ions (Musolff et al. 2015). Nutrient increases with increasing discharge at My Ly indicated the source was organic matter degradation in the forest area. Similar trends for the major ions at discharge were seen at Dua and Yen Thuong. Negative slopes were found for Ca^{2+}, Mg^{2+}, and HCO_3^- ($b = -0.12$ to -0.28) with low variability ($R^2 \geq 0.5$) and for Na^+ and SO_4^{2-} ($b = -0.13$ to -0.22) with moderate variability ($R^2 \geq 0.3$). The concentrations of NO_3^- and PO_4^{3-} were constant or increasing, indicating enrichment in nutrient sources in the basin (Musolff et al. 2015). Meanwhile, K^+ and Cl^- behaved chemostatically, increasing in the discharge at all basins, indicating important biogeochemical influences (Saunders and Lewis 1989) or exogenous sources (atmospheric deposition) (Musolff et al. 2015). For the major solutes (Ca^{2+}, Mg^{2+}, Na^+, and HCO_3^-), the dilution slopes at the downstream station were greater than those found midstream, indicating that catchments with higher water yields were more likely to express dilution (Moatar et al. 2017). The negative

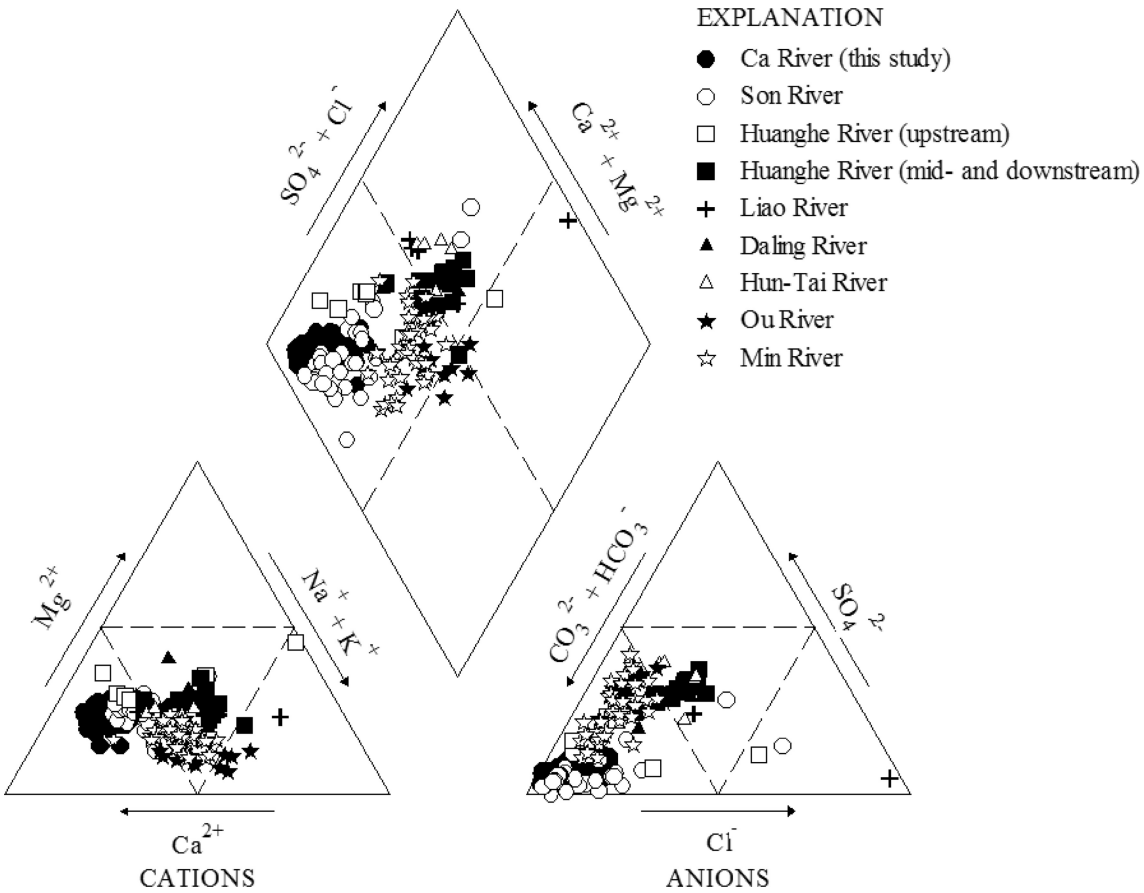

Fig. 6 Piper trilinear diagram of Ca River water in comparison with other river basins (data from Ding et al. 2016; Fan et al. 2014; Liu et al. 2018; Maharana et al. 2015)

correlation between major elements and runoff increased (higher R^2 values) with decreasing elevation (Torres et al. 2015). Less-reactive elements (Ca^{2+}, Mg^{2+}, and HCO_3^-) exhibited strong correlations with discharge and indicated various degrees of dilution with increasing runoff (Baronas et al. 2017). However, low correlations found for PO_4^{3-}, NO_3^-, Cl^-, and K^+ reflected biological processes, atmospheric input, or anthropogenic impacts (i.e., fertilizer application) (Bluth and Kump 1994; Moatar et al. 2017).

4.5 Primary evidence of reservoir impact on concentrations of suspended solids and dissolved solids

Located above the largest reservoir of the Ca River basin, My Ly is significantly influenced by the operation of the Ban Ve reservoir. The impact of water storage at the Ban Ve reservoir on the correlation between SSC and discharge at My Ly is shown in Fig. 8a. In August and September (the rainy season), SSC increased with increasing discharge. Water storage starts at the end of the rainy season (October), leading to increased water levels behind the reservoir. The water level was raised until it was over the My Ly station. Consequently, runoff was delayed during November and December. As a result, the SSC gradually decreased as suspended sediment settled, and sediment suspension was deferred during this period. The reservoir opened at the beginning of January, but SSC remained low until March because it was the dry season. Rain in April and May can wash out the settled sediment surrounding the upper part of My Ly, resulting in the steep increases in SSC. Thereafter, SSC increases with increasing discharge in June and July, consistent with increases seen in August and September.

Dua and Yen Thuong, located in the lower part of the main reservoirs in the Ca River basin, showed similar SSC behaviors in their discharges (Fig. 8b, c): decreasing SSCs with increasing discharge when comparing the rainy to dry seasons. This reflects the impact of suspended sediment settling in the reservoirs. Upstream sediment erosion also influenced that seen downstream; this is implied by the high SSC found in May. Generally, SSCs are positively correlated with streamflow (Moore and Anderholm 2002).

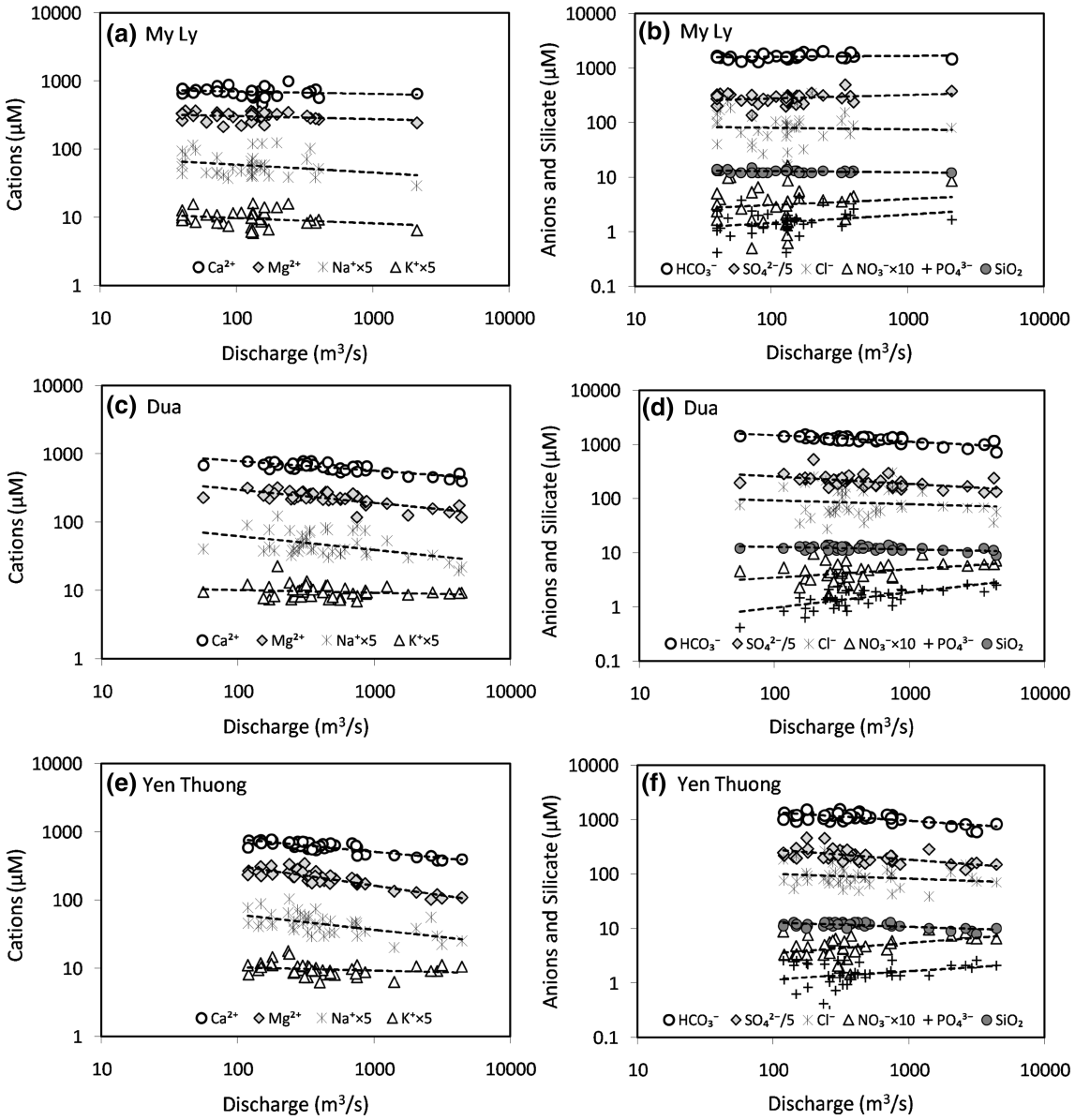

Fig. 7 Variation of river elements concentration with discharge at My Ly (**a**, **b**), Dua (**c**, **d**), and Yen Thuong (**e**, **f**)

However, reservoir operations lead to a variety of SSC behaviors in the discharge.

Dam closure not only affects suspended sediment but also river water quality (Muigai et al. 2010; Castilla-Hernandez et al. 2014). Variations in solute concentrations with discharge at My Ly were quite different from the fluxes with discharge at Dua and Yen Thuong. Differences could be the results of the impacts of the reservoir. During the wet season, when water is stored at My Ly, most ion concentrations were less variated than in other periods. When the reservoir was open, ion concentrations increased with discharge during the dry season until the highest concentration was reached at the first flash flood on 17 June 2018. Since then, ion concentrations decreased due to dilution. However, inverse correlations between ion concentrations and discharges were seen at Dua and Yen Thuong, indicating dilution effects (Zhang et al. 2015). When discharge exceeded 1000 m^3/s, ion concentrations decreased sharply, for example, on 17 December 2017, 8–12 October 2017, and 22 July 2018. The correlations between TSS and geochemical parameters are shown in Table 2 and indicate that suspended solids are negatively correlated with all ions (except NO_3^- and PO_4^{3-}) and TDS at Dua and Yen Thuong. This is common with increases in sediment, whereas chemical ions become diluted with increasing discharge. In contrast, positive correlations between TSS and K^+, Ca^{2+}, SO_4^{2-}, HCO_3^-, NO_3^-, PO_4^{3-}, and TDS were identified at My Ly. These results imply a

significant geochemical impact of water storage in the My Ly basin. When the water level at My Ly rises, My Ly can act as a reservoir, resulting in sediment suspension and sediment settling. Dam closures lead to increased water residence time, causing increased interaction between sediment particles and solutes. Dam closures also change the environmental water conditions (low oxygen content and high temperature), favoring biogeochemical processes (Moatar et al. 2017). Muigai et al. (2010) indicated that the reservoir leads to decreases in dissolved oxygen content due to eutrophication and increases the TDS value. Moore and Anderholm (2002) found that, in downstream reservoirs, TDS concentrations increase from evapotranspiration while nutrient concentrations decrease from settling and nutrient uptake, and SSCs decrease due to settling. In this study, it was not easy to assess the impact of the reservoir on the downstream basin because TDS values showed small seasonal variations. Moreover, the TDS concentration and composition were significantly influenced by multiple factors such as human activity, groundwater discharge, and tributary inflow. Therefore, the impact of dam closure on TDS in the downstream basin requires further investigation.

5 Conclusions

From 121 Ca River water samples collected from August 2017 to July 2018 at three stations, cations (Ca^{2+}, Mg^{2+}, Na^{+}, and K^{+}), anions (HCO_3^-, SO_4^{2-}, Cl^-, NO_3^-, and PO_4^{3-}), dissolved silica, SSCs, and TDS values showed that carbonate weathering is dominant. Bicarbonate and calcium are the prevailing chemical species, accounting for 84.4 and 62.0% of the total anionic and cationic charges, respectively. The TDS values varied from 77 to 205 mg/L, averaging 144 mg/L and decreasing in the downstream basin with decreases in major solute concentrations.

The relationships between solute concentrations and discharge show that the upstream catchment (My Ly) behaves chemostatically for the major chemical weathering products. Similar negative trends for Ca^{2+}, Mg^{2+}, HCO_3^-, Na^{+}, and SO_4^{2-} with discharge at Dua and Yen Thuong indicate dilution behaviors for those ions. The constant or increasing ion concentrations of NO_3^- and PO_4^{3-} in the three basins reflect enrichment of nutrients from organic matter degradation or human activity.

Relationships between SSC and discharge show that the reservoirs along the Ca River trigger sediment suspension and sediment settling at the My Ly station and decreasing SSCs at the Dua and Yen Thuong stations. Delays in water flow can lead to greater interactions between sediment and solutes and can allow biogeochemical processes that result in unusual changes in the concentrations of major ions and TDS with increasing discharges at My Ly.

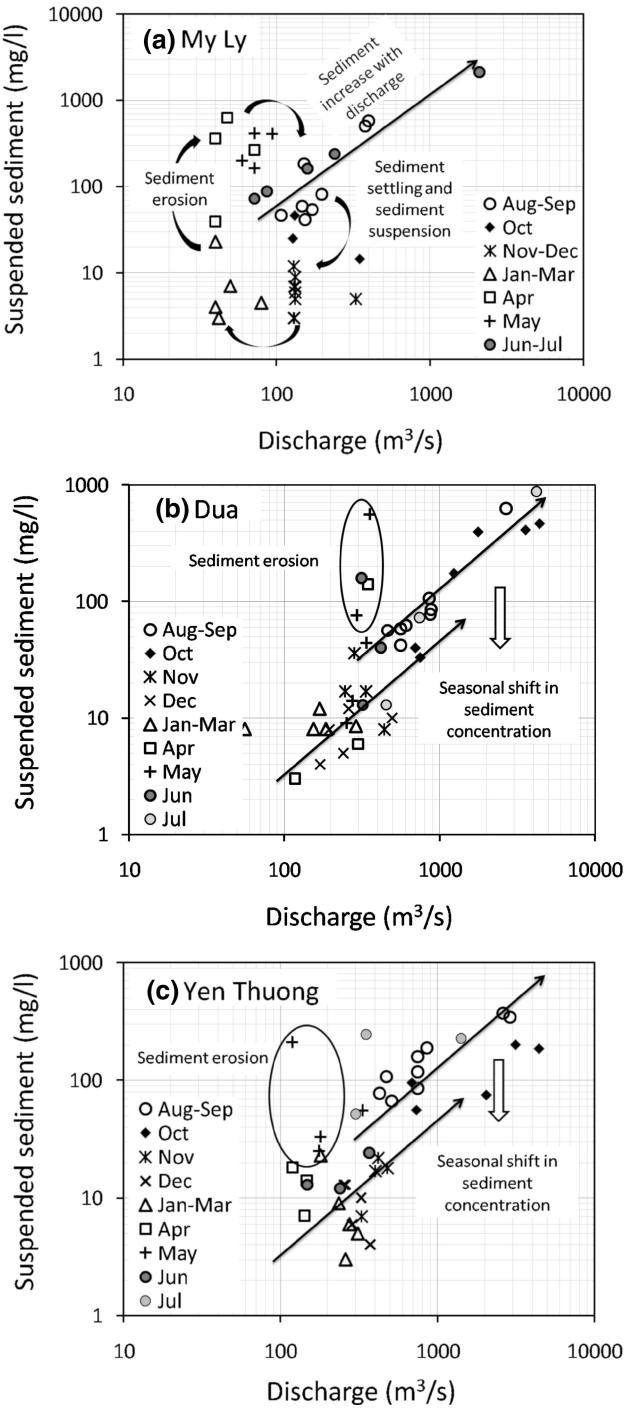

Fig. 8 Variation of suspended sediment concentration with discharge at My Ly (**a**), Dua (**b**) and Yen Thuong (**c**)

Acknowledgements This research was financially supported by the Japan Society for the Promotion of Science (Grant no. R11604). The authors would like to express their deep appreciation to Dr. Mitsuyo Saito of Graduate School Environmental and Life Science, Okayama University for her helpful comments on the manuscript and kind

support through the research process. The authors also thank staffs of North-Central Hydro-meteorological Centre, Vietnam for allowing us access to their gauging records. An anonymous reviewer is thanked for critically reading the manuscript and suggesting substantial improvements.

References

Amos P, Veale B, Thai NC, Read S (2017) Improving dam and downstream community safety in Vietnam. Hydropower Dams 1:37–43

Baronas JJ, Torres MA, Clark KE, West AJ (2017) Mixing as a driver of temporal variations in river hydrochemistry: 2. Major and trace element concentration dynamics in the Andes-Amazon transition. Water Resour Res 53(4):3120–3145. https://doi.org/10.1002/2016WR019729

Bluth GJS, Kump LR (1994) Lithologic and climatologic controls of river chemistry. Geochim Cosmochim Acta 58(10):2341–2359. https://doi.org/10.1016/0016-7037(94)90015-9

Bruijnzeel LA (1983) Hydrological and biogeochemical aspects of man-made forests in south-central Java, Indonesia. PhD Thesis, Vrije Universiteit, Amsterdam, p 256

Castilla-Hernandez P, del del R Torres-Alvarado M, Herrera-San Luis JA, Cruz-Lopez N (2014) Water quality of a reservoir and its major tributary located in east-central Mexico. Int J Environ Res Public Health 11(6):6119–6135. https://doi.org/10.3390/ijerph110606119

Chetelat B, Liu C-Q, Zhao ZQ, Wang QL, Li SL, Li J, Wang BL (2008) Geochemistry of the dissolved load of the Changjiang Basin rivers: anthropogenic impacts and chemical weathering. Geochim Cosmochim Acta 72(17):4254–4277. https://doi.org/10.1016/j.gca.2008.06.013

Chikamori H, Heng L, Daniel T (eds) (2012) Catalogue of rivers for Southeast Asia and the Pacific–Volume VI. UNESCO-IHP Regional Steering Committee for Southeast Asia and the Pacific. http://unesdoc.unesco.org/images/0021/002170/217039e.pdf

Ding H, Liu C-Q, Zhao Z-Q, Li S-L, Lang Y-C, Li X-D, Hu J, Liu B-J (2016) Geochemistry of the dissolved loads of the Liao River basin in northeast China under anthropogenic pressure: chemical weathering and controlling factors. J Asian Earth Sci 138:657–671. https://doi.org/10.1016/j.jseaes.2016.07.026

Fan B-L, Zhao Z-Q, Tao F-X, Liu B-J, Tao Z-H, Gao S, Zhang L-H (2014) Characteristics of carbonate, evaporite and silicate weathering in Huanghe River basin: a comparison among the upstream, midstream and downstream. J Asian Earth Sci 96:17–26. https://doi.org/10.1016/j.jseaes.2014.09.005

Gaillardet J, Dupre B, Allegre CJ, Negrel P (1997) Chemical and physical denudation in the Amazon River Basin. Chem Geol 142(3–4):141–173. https://doi.org/10.1016/s0009-2541(97)00074-0

Gibbs RJ (1970) Mechanisms controlling world water chemistry. Science 170(3962):1088–1090. https://doi.org/10.1126/science.170.3962.1088

Godsey SE, Kirchner JW, Clow DW (2009) Concentration–discharge relationships reflect chemostatic characteristics of US catchments. Hydrol Process 23(13):1844–1864. https://doi.org/10.1002/hyp.7315

Han G, Liu C (2001) Hydrogeochemistry of Wujiang River water in Guizhou province China. Chin J Geochem 20(3):240–248. https://doi.org/10.1007/BF03166145

Herndon EM, Dere AL, Sullivan PL, Norris D, Reynolds B, Brantley SL (2015) Landscape heterogeneity drives contrasting concentration–discharge relationships in shale headwater catchments. Hydrol Earth Syst Sci 19:3333–3347. https://doi.org/10.5194/hess-19-3333-2015

Holland HD (1978) The chemistry of the atmosphere and oceans. Wiley, Hoboken, p 351

Hunsaker CT, Johnson DW (2017) Concentration-discharge relationships in headwater streams of the Sierra Nevada, California. Water Resour Res 53(9):7869–7884. https://doi.org/10.1002/2016WR019693

IWRP (2012) Synthesis report of "Review of water resources planning in the Ca River basin" (in Vietnamese). Institute of Water Resources Planning, Directorate of Water Resources, Ha Noi

Ji H, Jiang Y (2012) Carbon flux and C, S isotopic characteristics of river waters from a karstic and a granitic terrain in the Yangtze River system. J Asian Earth Sci 57:38–53. https://doi.org/10.1016/j.jseaes.2012.06.004

Li S, Zhang Q (2008) Geochemistry of the upper Han River basin, China, 1: spatial distribution of major ion compositions and their controlling factors. Appl Geochem 23(12):3535–3544. https://doi.org/10.1016/j.apgeochem.2008.08.012

Li S, Xu Z, Wang H, Wang J, Zhang Q (2009) Geochemistry of the upper Han River basin, China 3: anthropogenic inputs and chemical weathering to the dissolved load. Chem Geol 264(1–4):89–95. https://doi.org/10.1016/j.chemgeo.2009.02.021

Liu W, Xu Z, Sun H, Zhao T, Shi C, Liu T (2018) Geochemistry of the dissolved loads of rivers in Southeast Coastal Region, China: anthropogenic impact on chemical weathering and carbon sequestration. Biogeosci Discuss. https://doi.org/10.5194/bg-2018-109 **(in review)**

Maharana C, Gautam SK, Singh AK, Tripathi JK (2015) Major ion chemistry of the Son River, India: weathering processes, dissolved fluxes and water quality assessment. J Earth Syst Sci 124(6):1293–1309. https://doi.org/10.1007/s12040-015-0599-0

Meybeck M (1987) Global chemical weathering of surficial rocks estimated from river dissolved loads. Am J Sci 287(5):401–428. https://doi.org/10.2475/ajs.287.5.401

Meybeck M (1994) Origin and variable composition of present day riverborne material. Material Fluxes on the Surface of the Earth. National Academic Press, Washington, DC, pp 61–73

Meybeck M, Helmer R (1989) The quality of rivers: from pristine stage to global pollution. Palaeogeogr Palaeoclimatol Palaeoecol 75(4):283–309. https://doi.org/10.1016/0031-0182(89)90191-0

Milliman JD, Farnsworth KL (2011) River discharge to the coastal ocean: a global synthesis. Cambridge University Press, Cambridge, p 384. https://doi.org/10.1017/CBO9780511781247

Moatar F, Abbott BW, Minaudo C, Curie F, Pinay G (2017) Elemental properties, hydrology, and biology interact to shape concentration-discharge curves for carbon, nutrients, sediment, and major ions. Water Resour Res 53(2):1270–1287. https://doi.org/10.1002/2016WR019635

Moon S, Huh Y, Qin J, Pho NV (2007) Chemical weathering in the Hong (Red) River basin: rates of silicate weathering and their controlling factors. Geochim Cosmochim Acta 71(6):1411–1430. https://doi.org/10.1016/j.gca.2006.12.004

Moore SJ, Anderholm SK (2002) Spatial and temporal variations in streamflow, dissolved solids, nutrients, and suspended sediment in the Rio Grande Valley study unit, Colorado, New Mexico, and Texas, 1993–95. US Geological Survey, National Water-Quality Assessment Program, Water-Resources Investigations Report 02-4224, Albuquerque, NM, 52 pp

Muigai PG, Shiundu PM, Mwaura FB, Kamau GN (2010) Correlation between dissolved oxygen and total dissolved solids and their role in the eutrophication of Nairobi dam, Kenya. Int J Bio Chem Phys 18:38–46

Musolff A, Schmidt C, Selle B, Fleckenstein JH (2015) Catchment controls on solute export. Adv Water Resour 86:133–146. https://doi.org/10.1016/j.advwatres.2015.09.026

Nauditt A, Ribbe L (eds) (2017) Land use and climate change interactions in central Vietnam. Water Resources and Development, Springer Book Series. https://doi.org/10.1007/978-981-10-2624-9

Negrel P, Roy S, Petelet-Giraud E, Millot R, Brenot A (2007) Long-term fluxes of dissolved and suspended matter in the Ebro River Basin (Spain). J Hydrol 342(3–4):249–260. https://doi.org/10.1016/j.jhydrol.2007.05.013

Roy S, Gaillardet J, Allegre CJ (1999) Geochemistry of dissolved and suspended loads of the Seine river, France: anthropogenic impact, carbonate and silicate weathering. Geochim Cosmochim Acta 63(9):1277–1292. https://doi.org/10.1016/s0016-7037(99)00099-x

Sarin MM, Krishnaswami S, Dilli K, Somayajulu BLK, Moore WS (1989) Major ion chemistry of the Ganga-Brahmaputra river system: weathering processes and fluxes to the Bay of Bengal. Geochim Cosmochim Acta 53(5):997–1009. https://doi.org/10.1016/0016-7037(89)90205-6

Saunders JF, Lewis WM (1989) Transport of major solutes and the relationship between solute concentrations and discharge in the Apure River. Venezuela. Biogeochemistry 8(2):101–113. https://doi.org/10.1007/BF00001315

Torres MA, West AJ, Clark KE (2015) Geomorphic regime modulates hydrologic control of chemical weathering in the Andes-Amazon. Geochim Cosmochim Acta 166:105–128. https://doi.org/10.1016/j.gca.2015.06.007

White AF, Blum AE (1995) Effects of climate on chemical weathering in watersheds. Geochim Cosmochim Acta 59(9):1729–1747. https://doi.org/10.1016/0016-7037(95)00078-E

Xiao J, Jin Z-D, Ding H, Wang J, Zhang F (2012) Geochemistry and solute sources of surface waters of the Tarim River Basin in the extreme arid region, NW Tibetan Plateau. J Asian Earth Sci 54–55:162–173. https://doi.org/10.1016/j.jseaes.2012.04.009

Zhang Q, Jin Z, Zhang F, Xiao J (2015) Seasonal variation in river water chemistry of the middle reaches of the Yellow River and its controlling factors. J Geochem Explor 156:101–113. https://doi.org/10.1016/j.gexplo.2015.05.008